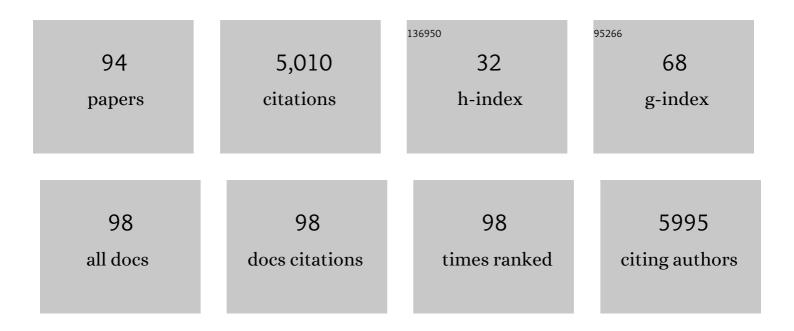
List of Publications by Year in descending order

Source: https://exaly.com/author-pdf/4345441/publications.pdf Version: 2024-02-01



DAWELLIANC

#	Article	IF	CITATIONS
1	Nanozyme: new horizons for responsive biomedical applications. Chemical Society Reviews, 2019, 48, 3683-3704.	38.1	1,101
2	DNA origami nanostructures can exhibit preferential renal uptake and alleviate acute kidney injury. Nature Biomedical Engineering, 2018, 2, 865-877.	22.5	297
3	Molybdenum-based nanoclusters act as antioxidants and ameliorate acute kidney injury in mice. Nature Communications, 2018, 9, 5421.	12.8	184
4	Ceria Nanoparticles Meet Hepatic Ischemiaâ€Reperfusion Injury: The Perfect Imperfection. Advanced Materials, 2019, 31, e1902956.	21.0	150
5	Magnetic Targeting of Nanotheranostics Enhances Cerenkov Radiation-Induced Photodynamic Therapy. Journal of the American Chemical Society, 2018, 140, 14971-14979.	13.7	148
6	Multiple-Armed Tetrahedral DNA Nanostructures for Tumor-Targeting, Dual-Modality in Vivo Imaging. ACS Applied Materials & Interfaces, 2016, 8, 4378-4384.	8.0	142
7	Bioresponsive Polyoxometalate Cluster for Redox-Activated Photoacoustic Imaging-Guided Photothermal Cancer Therapy. Nano Letters, 2017, 17, 3282-3289.	9.1	135
8	Bacteria-like mesoporous silica-coated gold nanorods for positron emission tomography and photoacoustic imaging-guided chemo-photothermal combined therapy. Biomaterials, 2018, 165, 56-65.	11.4	134
9	Tumor pH-responsive metastable-phase manganese sulfide nanotheranostics for traceable hydrogen sulfide gas therapy primed chemodynamic therapy. Theranostics, 2020, 10, 2453-2462.	10.0	120
10	Renalâ€Clearable PEGylated Porphyrin Nanoparticles for Imageâ€Guided Photodynamic Cancer Therapy. Advanced Functional Materials, 2017, 27, 1702928.	14.9	113
11	A Melaninâ€Based Natural Antioxidant Defense Nanosystem for Theranostic Application in Acute Kidney Injury. Advanced Functional Materials, 2019, 29, 1904833.	14.9	111
12	Seleniumâ€Doped Carbon Quantum Dots Act as Broadâ€5pectrum Antioxidants for Acute Kidney Injury Management. Advanced Science, 2020, 7, 2000420.	11.2	109
13	89Zr-labeled nivolumab for imaging of T-cell infiltration in a humanized murine model of lung cancer. European Journal of Nuclear Medicine and Molecular Imaging, 2018, 45, 110-120.	6.4	100
14	Ultra-small iron-gallic acid coordination polymer nanoparticles for chelator-free labeling of ⁶⁴ Cu and multimodal imaging-guided photothermal therapy. Nanoscale, 2017, 9, 12609-12617.	5.6	90
15	Self-Activated Electrical Stimulation for Effective Hair Regeneration <i>via</i> a Wearable Omnidirectional Pulse Generator. ACS Nano, 2019, 13, 12345-12356.	14.6	90
16	Dual-Modality Positron Emission Tomography/Optical Image-Guided Photodynamic Cancer Therapy with Chlorin e6-Containing Nanomicelles. ACS Nano, 2016, 10, 7721-7730.	14.6	88
17	Noninvasive PET Imaging of T cells. Trends in Cancer, 2018, 4, 359-373.	7.4	88
18	Reassembly of ⁸⁹ Zr‣abeled Cancer Cell Membranes into Multicompartment Membraneâ€Derived Liposomes for PETâ€Trackable Tumorâ€Targeted Theranostics. Advanced Materials, 2018, 30, e1704934.	21.0	86

#	Article	IF	CITATIONS
19	ImmunoPET Imaging of CTLA-4 Expression in Mouse Models of Non-small Cell Lung Cancer. Molecular Pharmaceutics, 2017, 14, 1782-1789.	4.6	84
20	Radiolabeling Silica-Based Nanoparticles via Coordination Chemistry: Basic Principles, Strategies, and Applications. Accounts of Chemical Research, 2018, 51, 778-788.	15.6	77
21	Chiralityâ€Ðriven Transportation and Oxidation Prevention by Chiral Selenium Nanoparticles. Angewandte Chemie - International Edition, 2020, 59, 4406-4414.	13.8	77
22	Renal-Clearable Ultrasmall Coordination Polymer Nanodots for Chelator-Free ⁶⁴ Cu-Labeling and Imaging-Guided Enhanced Radiotherapy of Cancer. ACS Nano, 2017, 11, 9103-9111.	14.6	73
23	Intrabilayer ⁶⁴ Cu Labeling of Photoactivatable, Doxorubicin-Loaded Stealth Liposomes. ACS Nano, 2017, 11, 12482-12491.	14.6	62
24	A head-to-head comparison of 68Ga-DOTA-FAPI-04 and 18F-FDG PET/MR in patients with nasopharyngeal carcinoma: a prospective study. European Journal of Nuclear Medicine and Molecular Imaging, 2021, 48, 3228-3237.	6.4	62
25	DNA nanomaterials for preclinical imaging and drug delivery. Journal of Controlled Release, 2016, 239, 27-38.	9.9	57
26	Nanomedicines for Renal Management: From Imaging to Treatment. Accounts of Chemical Research, 2020, 53, 1869-1880.	15.6	57
27	Intrathecal Administration of Nanoclusters for Protecting Neurons against Oxidative Stress in Cerebral Ischemia/Reperfusion Injury. ACS Nano, 2019, 13, 13382-13389.	14.6	53
28	Aptamer-Conjugated Framework Nucleic Acids for the Repair of Cerebral Ischemia-Reperfusion Injury. Nano Letters, 2019, 19, 7334-7341.	9.1	51
29	Radiolabeled polyoxometalate clusters: Kidney dysfunction evaluation and tumor diagnosis by positron emission tomography imaging. Biomaterials, 2018, 171, 144-152.	11.4	42
30	CD146â€Targeted Multimodal Imageâ€Guided Photoimmunotherapy of Melanoma. Advanced Science, 2019, 6, 1801237.	11.2	42
31	Constructing Higher-Order DNA Nanoarchitectures with Highly Purified DNA Nanocages. ACS Applied Materials & Materi	8.0	37
32	Chelator-Free Labeling of Metal Oxide Nanostructures with Zirconium-89 for Positron Emission Tomography Imaging. ACS Nano, 2017, 11, 12193-12201.	14.6	34
33	Noninvasive Imaging and Quantification of Radiotherapy-Induced PD-L1 Upregulation with ⁸⁹ Zr–Df–Atezolizumab. Bioconjugate Chemistry, 2019, 30, 1434-1441.	3.6	34
34	Efficient renal clearance of DNA tetrahedron nanoparticles enables quantitative evaluation of kidney function. Nano Research, 2019, 12, 637-642.	10.4	34
35	Prevention of Hepatic Ischemia-Reperfusion Injury by Carbohydrate-Derived Nanoantioxidants. Nano Letters, 2020, 20, 6510-6519.	9.1	32
36	Radiolabeled pertuzumab for imaging of human epidermal growth factor receptor 2 expression in ovarian cancer. European Journal of Nuclear Medicine and Molecular Imaging, 2017, 44, 1296-1305.	6.4	31

#	Article	IF	CITATIONS
37	ImmunoPET imaging of CD38 in murine lymphoma models using 89Zr-labeled daratumumab. European Journal of Nuclear Medicine and Molecular Imaging, 2018, 45, 1372-1381.	6.4	30
38	Ultrasmall Porous Silica Nanoparticles with Enhanced Pharmacokinetics for Cancer Theranostics. Nano Letters, 2021, 21, 4692-4699.	9.1	30
39	Extracellular vesicles-based pre-targeting strategy enables multi-modal imaging of orthotopic colon cancer and image-guided surgery. Journal of Nanobiotechnology, 2021, 19, 151.	9.1	29
40	Synthesis and evaluation of 18F-labeled bile acid compound: A potential PET imaging agent for FXR-related diseases. Nuclear Medicine and Biology, 2014, 41, 495-500.	0.6	28
41	CD38 as a PET Imaging Target in Lung Cancer. Molecular Pharmaceutics, 2017, 14, 2400-2406.	4.6	25
42	ImmunoPET for assessing the differential uptake of a CD146-specific monoclonal antibody in lung cancer. European Journal of Nuclear Medicine and Molecular Imaging, 2016, 43, 2169-2179.	6.4	23
43	[^{nat/44} Sc(pypa)] ^{â^'} : Thermodynamic Stability, Radiolabeling, and Biodistribution of a Prostate-Specific-Membrane-Antigen-Targeting Conjugate. Inorganic Chemistry, 2020, 59, 1985-1995.	4.0	23
44	Advances in aptamer-based nuclear imaging. European Journal of Nuclear Medicine and Molecular Imaging, 2022, 49, 2544-2559.	6.4	23
45	Chiralityâ€Driven Transportation and Oxidation Prevention by Chiral Selenium Nanoparticles. Angewandte Chemie, 2020, 132, 4436-4444.	2.0	22
46	Tissue Factor‶argeted ImmunoPET Imaging and Radioimmunotherapy of Anaplastic Thyroid Cancer. Advanced Science, 2020, 7, 1903595.	11.2	22
47	Noninvasive Evaluation of CD20 Expression Using ⁶⁴ Cu-Labeled F(ab′) ₂ Fragments of Obinutuzumab in Lymphoma. Journal of Nuclear Medicine, 2021, 62, 372-378.	5.0	21
48	Radionuclide-based molecular imaging allows CAR-T cellular visualization and therapeutic monitoring. Theranostics, 2021, 11, 6800-6817.	10.0	21
49	Spherical nucleic acids: Organized nucleotide aggregates as versatile nanomedicine. Aggregate, 2022, 3, e120.	9.9	21
50	CD38â€Targeted Theranostics of Lymphoma with ⁸⁹ Zr/ ¹⁷⁷ Luâ€Labeled Daratumumab. Advanced Science, 2021, 8, 2001879.	11.2	20
51	Intracellular signaling pathway in dendritic cells and antigen transport pathway in vivo mediated by an OVA@DDAB/PLGA nano-vaccine. Journal of Nanobiotechnology, 2021, 19, 394.	9.1	20
52	Noninvasive Trafficking of Brentuximab Vedotin and PET Imaging of CD30 in Lung Cancer Murine Models. Molecular Pharmaceutics, 2018, 15, 1627-1634.	4.6	19
53	86/90Y-Based Theranostics Targeting Angiogenesis in a Murine Breast Cancer Model. Molecular Pharmaceutics, 2018, 15, 2606-2613.	4.6	19
54	86/90Y-Labeled Monoclonal Antibody Targeting Tissue Factor for Pancreatic Cancer Theranostics. Molecular Pharmaceutics, 2020, 17, 1697-1705.	4.6	19

#	Article	IF	CITATIONS
55	Escherichiacoli Nissle 1917 as a Novel Microrobot for Tumor-Targeted Imaging and Therapy. Pharmaceutics, 2021, 13, 1226.	4.5	19
56	Antibody and fragment-based PET imaging of CTLA-4+ T-cells in humanized mouse models. American Journal of Cancer Research, 2019, 9, 53-63.	1.4	19
57	Radiolabeling of DNA Bipyramid and Preliminary Biological Evaluation in Mice. Bioconjugate Chemistry, 2016, 27, 905-910.	3.6	18
58	ImmunoPET of trophoblast cell-surface antigen 2 (Trop-2) expression in pancreatic cancer. European Journal of Nuclear Medicine and Molecular Imaging, 2022, 49, 861-870.	6.4	18
59	Targeting angiogenesis for radioimmunotherapy with a 177Lu-labeled antibody. European Journal of Nuclear Medicine and Molecular Imaging, 2018, 45, 123-131.	6.4	17
60	Nanostructured polyvinylpyrrolidone-curcumin conjugates allowed for kidney-targeted treatment of cisplatin induced acute kidney injury. Bioactive Materials, 2023, 19, 282-291.	15.6	17
61	Multi-antitumor therapy and synchronous imaging monitoring based on exosome. European Journal of Nuclear Medicine and Molecular Imaging, 2022, 49, 2668-2681.	6.4	16
62	ImmunoPET Imaging of CD146 in Murine Models of Intrapulmonary Metastasis of Non-Small Cell Lung Cancer. Molecular Pharmaceutics, 2017, 14, 3239-3247.	4.6	15
63	A Switchable Site-Specific Antibody Conjugate. ACS Chemical Biology, 2018, 13, 958-964.	3.4	15
64	Salinomycin nanocrystals for colorectal cancer treatment through inhibition of Wnt/\hat{l}^2 -catenin signaling. Nanoscale, 2020, 12, 19931-19938.	5.6	15
65	Development and characterization of CD54-targeted immunoPET imaging in solid tumors. European Journal of Nuclear Medicine and Molecular Imaging, 2020, 47, 2765-2775.	6.4	15
66	Conductive nanocomposite hydrogel and mesenchymal stem cells for the treatment of myocardial infarction and non-invasive monitoring via PET/CT. Journal of Nanobiotechnology, 2022, 20, 211.	9.1	15
67	ImmunoPET/NIRF/Cerenkov multimodality imaging of ICAM-1 in pancreatic ductal adenocarcinoma. European Journal of Nuclear Medicine and Molecular Imaging, 2021, 48, 2737-2748.	6.4	14
68	Nectin-4-targeted immunoSPECT/CT imaging and photothermal therapy of triple-negative breast cancer. Journal of Nanobiotechnology, 2022, 20, .	9.1	14
69	Fluorine-18 labeling by click chemistry: Multiple probes in one pot. Applied Radiation and Isotopes, 2013, 75, 64-70.	1.5	13
70	ImmunoPET of CD146 in Orthotopic and Metastatic Breast Cancer Models. Bioconjugate Chemistry, 2021, 32, 1306-1314.	3.6	13
71	ImmunoPET Imaging of TIMâ€3 in Murine Melanoma Models. Advanced Therapeutics, 2020, 3, 2000018.	3.2	12
72	64Cu-labeled daratumumab F(ab′)2 fragment enables early visualization of CD38-positive lymphoma. European Journal of Nuclear Medicine and Molecular Imaging, 2022, 49, 1470-1481.	6.4	12

#	Article	IF	CITATIONS
73	Minimizing adverse effects of Cerenkov radiation induced photodynamic therapy with transformable photosensitizer-loaded nanovesicles. Journal of Nanobiotechnology, 2022, 20, 203.	9.1	12
74	Dual-labeled pertuzumab for multimodality image-guided ovarian tumor resection. American Journal of Cancer Research, 2019, 9, 1454-1468.	1.4	11
75	Radiolabeling of RGD peptide and preliminary biological evaluation in mice bearing U87MG tumors. Bioorganic and Medicinal Chemistry, 2012, 20, 3850-3855.	3.0	10
76	HER2-targeted multimodal imaging of anaplastic thyroid cancer. American Journal of Cancer Research, 2019, 9, 2413-2427.	1.4	10
77	ImmunoPET imaging of CD38 expression in hepatocellular carcinoma using Cu-labeled daratumumab. American Journal of Translational Research (discontinued), 2019, 11, 6007-6015.	0.0	8
78	Multifunctional flexible contact lens for eye health monitoring using inorganic magnetic oxide nanosheets. Journal of Nanobiotechnology, 2022, 20, 202.	9.1	8
79	Framework Nucleic Acids in Nuclear Medicine Imaging: Shedding Light on Nano–Bio Interactions. Angewandte Chemie - International Edition, 2022, 61, .	13.8	7
80	lmmuno-PET imaging of VEGFR-2 expression in prostate cancer with Zr-labeled ramucirumab. American Journal of Cancer Research, 2019, 9, 2037-2046.	1.4	7
81	Spatiotemporal Distribution of Agrin after Intrathecal Injection and Its Protective Role in Cerebral Ischemia/Reperfusion Injury. Advanced Science, 2020, 7, 1902600.	11.2	5
82	Incremental Value of Left Ventricular Mechanical Dyssynchrony Assessment by Nitrogen-13 Ammonia ECG-Gated PET in Patients With Coronary Artery Disease. Frontiers in Cardiovascular Medicine, 2021, 8, 719565.	2.4	3
83	Mapping COVID-19 with nuclear imaging: from infection to functional sequelae. American Journal of Nuclear Medicine and Molecular Imaging, 2021, 11, 59-63.	1.0	3
84	Labeling of Erythrocytes by Porphyrinâ€Phospholipid. Advanced NanoBiomed Research, 2021, 1, 2000013.	3.6	2
85	Framework Nucleic Acids in Nuclear Medicine Imaging: shedding light on nanoâ€bio interactions. Angewandte Chemie, 0, , .	2.0	2
86	New wine in old bottles: Ga-PSMA-11 PET/CT reveals COVID-19 in patients with prostate cancer. American Journal of Nuclear Medicine and Molecular Imaging, 2021, 11, 332-336.	1.0	2
87	Frontispiece: Chiralityâ€Driven Transportation and Oxidation Prevention by Chiral Selenium Nanoparticles. Angewandte Chemie - International Edition, 2020, 59, .	13.8	1
88	Visualizing Cytokeratin-14 Levels in Basal-Like Breast Cancer via ImmunoSPECT Imaging. Molecular Pharmaceutics, 2022, 19, 3542-3550.	4.6	1
89	Frontispiz: Chiralityâ€Ðriven Transportation and Oxidation Prevention by Chiral Selenium Nanoparticles. Angewandte Chemie, 2020, 132, .	2.0	0
90	High-performance renal imaging with a radiolabeled, non-excretable chimeric fusion protein. Theranostics, 2021, 11, 9177-9179.	10.0	0

#	Article	IF	CITATIONS
91	[18F]F-ET-OTSSP167 Targets Maternal Embryo Leucine Zipper Kinase for PET Imaging of Triple-Negative Breast Cancer. Molecular Pharmaceutics, 2021, 18, 3544-3552.	4.6	0
92	é~´ç¦»åäºæ¢è‰²è°±åœ¨DNA纳米结构纯åŒ−ä,的应甔. Scientia Sinica Chimica, 2015, 45, 1220-1225.	0.4	0
93	ImmunoPET of the differential expression of CD146 in breast cancer. American Journal of Cancer Research, 2021, 11, 1586-1599.	1.4	Ο
94	Glomerular filtration rate calculation based on Ga-EDTA dynamic renal PET American Journal of Nuclear Medicine and Molecular Imaging, 2022, 12, 54-62.	1.0	0